

Effects of magnetic doping and temperature dependence of phonon dynamics in $\text{CaFe}_{1-x}\text{Co}_x\text{AsF}$ compounds ($x=0, 0.06, \text{ and } 0.12$)

R. Mittal,^{1,2} M. Zbiri,³ S. Rols,³ Y. Su,¹ Y. Xiao,⁴ H. Schober,³ S. L. Chaplot,² M. Johnson,³ T. Chatterji,⁵ S. Matsuishi,⁶ H. Hosono,⁶ and Th. Brueckel^{1,4}

¹Juelich Centre for Neutron Science, IFF, Forschungszentrum Juelich Outstation at FRM II, Lichtenbergstr. 1, D-85747 Garching, Germany

²Solid State Physics Division, Bhabha Atomic Research Centre, Trombay, Mumbai 400085, India

³Institut Laue-Langevin, BP 156, 38042 Grenoble Cedex 9, France

⁴Institut fuer Festkoerperforschung, Forschungszentrum Juelich, D-52425 Juelich, Germany

⁵Juelich Centre for Neutron Science, Forschungszentrum Juelich Outstation at Institut Laue-Langevin, BP 156, 38042 Grenoble Cedex 9, France

⁶Frontier Research Center, Tokyo Institute of Technology, 4259 Nagatsuta-cho, Midori-ku, Yokohama 226-8503, Japan
(Received 22 April 2009; revised manuscript received 21 May 2009; published 12 June 2009)

We report detailed measurements of composition as well as temperature dependence of the phonon density of states in a new series of FeAs compounds with composition $\text{CaFe}_{1-x}\text{Co}_x\text{AsF}$ ($x=0, 0.06, 0.12$). The electronic-structure calculations for these compounds show that bands near the Fermi level are mainly formed by Fe 3d states, which is quite different from other 122 and 1111 FeAs compounds where both Fe and As are believed to be related to superconductivity. The difference in electronic structure for fluorine-based compounds may cause phonon spectra to behave differently as a function of composition and temperature in comparison with our previous phonon studies on parent and superconducting $M\text{Fe}_2\text{As}_2$ ($M=\text{Ba}, \text{Ca}, \text{Sr}$). The composition as well as temperature dependence of phonon spectra for $\text{CaFe}_{1-x}\text{Co}_x\text{AsF}$ ($x=0, 0.06, 0.12$) compounds have been measured using time-of-flight IN4C and IN6 spectrometers at Institut Laue Langevin, France. The comparison of phonon spectra at 300 K in these compounds shows that acoustic phonon modes up to 12 meV harden in the doped compounds in comparison to the parent CaFeAsF . While intermediate-energy phonon modes from 15 to 25 meV are also found to shift toward high energies only in the 12% Co-doped CaFeAsF compound. The experimental results for $\text{CaFe}_{1-x}\text{Co}_x\text{AsF}$ ($x=0, 0.06, 0.12$) are quite different from our previous phonon studies on parent and superconducting $M\text{Fe}_2\text{As}_2$ ($M=\text{Ba}, \text{Ca}, \text{Sr}$) where low-energy acoustic phonon modes do not react with doping, while the phonon spectra in the intermediate range from 15 to 25 meV are found to soften in these compounds. We argue that stronger spin phonon interaction play an important role in the emergence of superconductivity in these compounds. The lattice dynamics of $\text{CaFe}_{1-x}\text{Co}_x\text{AsF}$ ($x=0, 0.06, 0.12$) compounds is also investigated using the *ab initio* as well as shell-model phonon calculations. We show that the nature of the interaction between the Ca and the Fe-As layers in CaFeAsF compounds is quite different compared to our previous studies on CaFe_2As_2 .

DOI: [10.1103/PhysRevB.79.214514](https://doi.org/10.1103/PhysRevB.79.214514)

PACS number(s): 74.25.Kc, 78.70.Nx, 63.20.-e

I. INTRODUCTION

The discovery of superconductivity in La-based FeAs ($T_c=26$ K) compound has stimulated enormous interest¹⁻²⁸ in the field of condensed-matter physics. There are mainly three types of FeAs-based superconductors such as $R\text{FeAsO}$ (R : rare-earth elements), $A\text{Fe}_2\text{As}_2$ (A : alkaline-earth elements), and LiFeAs . The structural, magnetic, and electronic properties of all the compounds have been extensively investigated to understand the mechanism of superconductivity. In particular, for all these compounds, strong anomalies have been found¹⁻⁵ in the specific heat, resistivity, and magnetic susceptibility in the temperature range of 110–180 K. These anomalies are now known to be a prerequisite for superconductivity in FeAs compounds. In addition, it should be noted that recent results suggest that superconductivity and magnetism coexists^{6,7} in these compounds.

Research groups are continuously making efforts to synthesize new FeAs compounds with higher T_c . Very recently, new oxygen-free FeAs compounds $M\text{FeAsF}$ ($M=\text{Sr}, \text{Ca}, \text{ and } \text{Eu}$) with ZrCuSiAs -type phase have been synthesized.⁹⁻¹⁴

These new compounds are analogous to $R\text{FeAsO}$, where the $(RO)^+$ layer is replaced by $(MF)^+$ layer. Spin-density wave anomalies have been found¹² in CaFeAsF and SrFeAsF at about 118 and 180 K, respectively. The bulk superconductivity at 56 and 32 K has been found¹⁰ in SrFeAsF on partial substitution of Sr by Sm and La, respectively. For CaFeAsF , the Co and Ni doping on the Fe site induces the superconductivity¹³ with a T_c of 22 and 12 K, respectively, while the discovery of superconductivity has been reported¹⁴ in $\text{Ca}_{0.4}\text{R}_{0.6}\text{FeAsF}$ ($R=\text{Nd}, \text{Pr}$) with T_c of 57.4 and 52.8 K by doping of Nd and Pr, respectively.

Neutron powder-diffraction experiments have been carried out¹⁵ to investigate the structural-phase transition as well as magnetic order in $\text{CaFe}_{1-x}\text{Co}_x\text{AsF}$ compounds ($x=0, 0.06, 0.12$). In this context, the relation between superconductivity, magnetic behavior, and structural instabilities have been studied. Resonant-spin excitations have been observed¹⁶ in a number of FeAs compounds by inelastic neutron scattering. Both inelastic neutron-scattering and first-principles electronic-band-structure calculations indicate that superconductivity in the FeAs-based compounds is uncon-

ventional and might be mediated by magnetic spin fluctuations.¹⁷ The suppression of the magnetic ordering giving rise to superconductivity requires lattice excitations leading to a coupling of the magnetic and structural degrees of freedom. Hence, it is important to experimentally measure the phonon excitations and search for specific features in the phonon spectra. Raman spectra¹⁸ of nonsuperconducting CaFe_2As_2 and SrFe_2As_2 and superconducting $\text{Sr}_{0.6}\text{K}_{0.4}\text{Fe}_2\text{As}_2$ have been measured.

Inelastic x-ray scattering has been used to investigate¹⁹ the phonon density of states in $\text{LaFeAsO}_{1-x}\text{F}_x$ and NdFeAsO . Only very few phonon studies have been reported^{19,20} for single crystals of BaFe_2As_2 and PrFeAsO_{1-y} using inelastic x-ray scattering. *Ab initio* phonon calculations and shell-model calculations have been used to calculate the phonon spectrum of these compounds. We have also investigated these compounds using the technique of inelastic neutron scattering from polycrystalline samples^{21–24} of BaFe_2As_2 , CaFe_2As_2 , $\text{Sr}_{0.6}\text{K}_{0.4}\text{Fe}_2\text{As}_2$, and $\text{Ca}_{0.6}\text{Na}_{0.4}\text{Fe}_2\text{As}_2$ and a single crystal²⁵ of CaFe_2As_2 .

The valence-band electrons close to the Fermi surface are mainly believed to be involved in the superconductivity. The electronic-structure calculation²⁶ for $M\text{FeAsF}$ shows that bands near the Fermi level are mainly formed by Fe $3d$ states. The Fe partial density of states at the Fermi level increases on going from SrFeAsF to CaFeAsF . This is quite different from $R\text{FeAsO}$ and $M\text{Fe}_2\text{As}_2$ (M : Alkaline-earth elements) compounds where bonding and interaction of both Fe and As are believed to be responsible for superconductivity. We are conducting systematic studies of the temperature as well as composition dependence of phonon spectra for FeAs compounds. It is of interest to investigate the phonon spectrum of FeAs compounds as a function of increase in dopant concentration. In this continuation of our studies on FeAs compounds we now report the experimental temperature dependence of phonon spectra for $\text{CaFe}_{1-x}\text{Co}_x\text{AsF}$ ($x=0,0.06,0.12$) compounds. Phonons have also been estimated by means of lattice-dynamics calculations in order to analyze the observed spectra. The details about the experimental and lattice-dynamical techniques are given in Secs. II and III, respectively. The obtained results are given in Sec. IV. Finally Sec. V is dedicated to the conclusions.

II. EXPERIMENTAL

The polycrystalline samples of CaFeAsF , $\text{CaFe}_{0.94}\text{Co}_{0.06}\text{AsF}$ (onset $T_c=20$ K), and $\text{CaFe}_{0.88}\text{Co}_{0.12}\text{AsF}$ ($T_c=20$ K) were prepared¹² by solid-state synthesis techniques. All the samples were extensively characterized¹⁵ by the means of neutron powder diffraction, dc magnetization, and electrical resistivity and confirmed their high quality. The neutron powder-diffraction measurements were performed on the high-flux powder diffractometer D20 at Institut Laue Langevin (ILL) (Grenoble, France). Rietveld refinement of the diffraction data indicates that samples contain small impurity phases (CaF_2 and Fe_2O_3) of less than 1%. The details about the characterization of our samples are given in our previous publication.¹⁵

The inelastic neutron-scattering experiments were performed using the IN4C and IN6 time-of-flight spectrometers

at the Institut Laue Langevin, France. An incident neutron wavelength of 1.1 \AA (67.6 meV) was chosen for the IN4C measurements which allowed the data collection in the neutron-energy-loss mode. The measurements for $\text{CaFe}_{1-x}\text{Co}_x\text{AsF}$ compounds ($x=0,0.06,0.12$) using the IN4C spectrometer were carried out at 2, 125, and 150 K. The tetragonal-to-orthorhombic phase transition in $\text{CaFe}_{0.94}\text{Co}_{0.06}\text{AsF}$ is determined to be at around 85(3) K. So for the $x=0.06$ compound we have collected one more data set at 50 K. The high-resolution data for all the three compounds at 300 K were also collected using IN6. For these measurements we have used an incident neutron wavelength of 5.1 \AA (3.12 meV). The full energy range of the phonon spectra at IN6 can only be covered by performing measurements in the neutron-energy-gain mode. In the incoherent one-phonon approximation the measured scattering function $S(Q, E)$, as observed in the neutron experiments, is related²⁹ to the phonon density of states $g^{(n)}(E)$ as follows:

$$g^{(n)}(E) = A \left\langle \frac{e^{2W_k(Q)}}{Q^2} \frac{E}{n(E, T) + \frac{1}{2} \pm \frac{1}{2}} S(Q, E) \right\rangle, \quad (1)$$

$$g^n(E) = B \sum_k \left\{ \frac{4\pi b_k^2}{m_k} \right\} g_k(E), \quad (2)$$

where the + or – signs correspond to energy loss or gain of the neutrons, respectively, and where $n(E, T) = [\exp(E/k_B T) - 1]^{-1}$. A and B are normalization constants and b_k , m_k , and $g_k(E)$ are, respectively, the neutron-scattering length, mass, and partial density of states of the k th atom in the unit cell. The quantity between $\langle \rangle$ represents suitable average over all Q values at a given energy. $2W(Q)$ is the Debye-Waller factor. The weighting factors $\frac{4\pi b_k^2}{m_k}$ for various atoms in the units of barns/amu are Ca=0.071; Fe=0.208 and As=0.073; F=0.211; Co=0.095. The values of neutron-scattering lengths for various atoms can be found from Ref. 30. The experimental phonon data is always contaminated by the multiphonon contribution. In order to compare the experimental data with the calculated one-phonon spectra, one has to subtract the multiphonon contribution from the measured phonon spectra at each temperature. We have calculated multiphonon contribution by Sjolander formalism³¹ and subtracted it from the experimental data.

III. LATTICE-DYNAMICAL CALCULATIONS

We have measured temperature dependence of phonon spectra for $\text{CaFe}_{1-x}\text{Co}_x\text{AsF}$ ($x=0,0.06,0.12$) compounds. The calculation of phonon spectra are needed for interpretation of the experimental data. For CaFeAsF we have made an attempt to develop an interatomic potential model. Further, density-functional theory (DFT) calculations have been undertaken to derive the phonon frequencies.

The lattice-dynamical calculation is performed^{32,33} using the following interatomic potentials:

$$V(r) = \left\{ \frac{e^2}{4\pi\epsilon_0} \right\} \left\{ \frac{Z(k)Z(k')}{r} \right\} + a \exp \left\{ \frac{-br}{R(k) + R(k')} \right\} - \frac{C}{r^6} - D \exp[-n(r - r_0)^2/(2r)], \quad (3)$$

where r is the distance between the atoms k and k' . The first term is the long-range Coulombic attractive potential, the second is the Born-Mayer repulsion, and the third is the van der Waals attraction potential. The parameters of the interatomic potential are the effective charge $Z(K)$ and radius $R(k)$ of the atom type k . $1/(4\pi\epsilon_0) = 9 \times 10^9 \text{ Nm}^2/\text{Coul}^2$, $a = 1822 \text{ eV}$, and $b = 12.364$. The third term in Eq. (3) is applied only between Fe-As and As-As atoms. The radii parameters used in our calculations are $R(\text{Ca}) = 2.18 \text{ \AA}$, $R(\text{Fe}/\text{Co}) = 0.42 \text{ \AA}$, $R(\text{As}) = 2.59 \text{ \AA}$, and $R(\text{F}) = 1.22 \text{ \AA}$. Partial charges of $Z(\text{Ca}) = 2.00$, $Z(\text{Fe}/\text{Co}) = 0.30$, $Z(\text{As}) = -1.35$, and $Z(\text{F}) = -0.95$ are used in the calculations. The parameter C was set to $C(\text{Fe-As}) = 70 \text{ eV/\AA}$ (Ref. 6) and $C(\text{F-F}) = 107 \text{ eV/\AA}$.⁶ The covalent nature of the Fe-As bond has been described by further including the stretching potential given by the fourth term in Eq. (3). The parameters of the stretching potential are $D = 2.40 \text{ eV}$, $n = 9.2 \text{ \AA}^{-1}$, and $r_0 = 2.395 \text{ \AA}$.

The polarizability of the As and F atoms is introduced in the framework of the shell model³⁴ with the shell charge $Y(\text{As}) = -1.45$ and $Y(\text{F}) = -1.00$, and shell-core force constant $K(\text{As}) = 40 \text{ eV/\AA}^2$ and $K(\text{F}) = 150 \text{ eV/\AA}^2$. Due to the metallic nature of FeAs compounds, the screened Coulomb potential in the Thomas-Fermi approximation was used for the calculations. The screening parameter $k_o = 0.35 \text{ \AA}^{-1}$ has been used in our calculations. The code³⁵ “DISPR” developed at Trombay is used for the calculation of phonon frequencies and polarization vector of the phonons in the entire Brillouin zone.

Further, DFT-based first-principles calculations were performed using the projector-augmented wave (PAW) formalism³⁶ of the Kohn-Sham DFT (Refs. 37 and 38) at the generalized gradient approximation (GGA) level, implemented in the Vienna *ab initio* simulation package (VASP) (Refs. 39 and 40). The GGA was formulated by the Perdew-Burke-Ernzerhof (PBE) (Refs. 41 and 42) density functional. The Gaussian broadening technique was adopted and all results are well converged with respect to k mesh and energy cutoff for the plane-wave expansion. Experimentally refined crystallographic data in the low temperature has been considered. This structure was used to calculate the generalized density of states (GDOS) and dispersion relations for the base-centered orthorhombic phase under the *Cmma* space group (number 67) having the local point-group symmetry D_{21}^{2h} . In case of CaFeAsF, the Fe moments are parallel to the longer a axis. Spins are aligned ferromagnetically along the shorter b axis and antiferromagnetically along the a and c axes. In order to take into account computationally the observed magnetic ordering, one has to double the cell along the c axis to get two layers of Fe cations and hence an antiferromagnetic ordering along this direction. This is specific to the present system when compared to the other FeAs-based compounds, having two Fe layers without doubling along c axis. In the lattice-dynamics calculations, in order to

determine all interatomic-force constants, the supercell approach has been adopted.⁴³ Therefore, the single cell was used to construct a (2^*a , 2^*b , 2^*c) supercell containing 32 f.u. (128 atoms), a and b being the shorter cell axes. Total energies and interatomic forces were calculated for the 24 structures resulting from individual displacements of the four symmetry-inequivalent atoms, along the three inequivalent Cartesian directions ($\pm x$, $\pm y$, and $\pm z$). The 24 phonon branches corresponding to the 8 atoms in the primitive cell were extracted in subsequent calculations using the PHONON software.⁴⁴ In the followings, magnetic means that the supercell has been doubled along the c axis ($2 \times 2 \times 2$) to get two Fe layers (128 atoms) whereas nonmagnetic phonons refer to calculations without doubling along the c axis (supercell, $2 \times 2 \times 1$, 64 atoms), i.e., no magnetism is considered.

By remaining in space group 67, the magnetic calculation described above results in a averaging of the magnetic interactions in the dynamical matrix constructed in the PHONON software.⁴⁴ In order to include the precise ferromagnetic (b direction) and antiferromagnetic (a and c directions) ordering in the dynamical matrix, the space-group symmetry has to be changed and a second Fe site has to be introduced. Antiferromagnetic ordering in the a direction reduces the symmetry to *Pmma* (49) but including the ordering in the c direction raises the symmetry to *Ibam* (72), which is associated with a doubling of the unit cell. We refer to this more detailed magnetic calculation as the “broken-symmetry” approach.

IV. RESULTS AND DISCUSSION

A. Comparison of phonon spectra for CaFe_{1-x}Co_xAsF compounds ($x=0, 0.06, 0.12$)

The high-resolution density-of-states measurements for CaFe_{1-x}Co_xAsF compounds ($x=0, 0.06, 0.12$) measured at 300 K using the IN6 spectrometer are shown in Fig. 1. The structural and magnetic transition in these compounds is below 134 K. The measurements on IN6 can only be performed with a small incident neutron energy of 3.12 meV in the neutron-energy-gain mode, which does not give enough intensity at low temperatures. We have carried out density-of-states measurements only at 300 K. These measurements, carried out with very high elastic-energy resolution of about 200 μeV (inelastic focusing mode), show that low-energy phonon modes below 12 meV harden on doping of 6% of Co at the Fe site (Fig. 1). A further increase in the Co concentration to 12% does not seem to affect the low-energy phonon spectra. However, the intermediate-energy phonon modes from 18 to 25 meV also harden in addition to the acoustic modes on 12% Co doping in comparison to the parent and 6% Co-doped compounds.

The calculated partial density of states (Fig. 2) of various atoms (Sec. IV C) in CaFe_{1-x}Co_xAsF compounds ($x=0, 0.06, 0.12$) show that at low energies below 12 meV the contribution to phonon spectra is mainly from the Fe_{1-x}Co_x or As sublattice. The shell-model calculation (Sec. IV C) which does not consider the effect of electron-phonon coupling influence on the phonon spectra shows that the partial

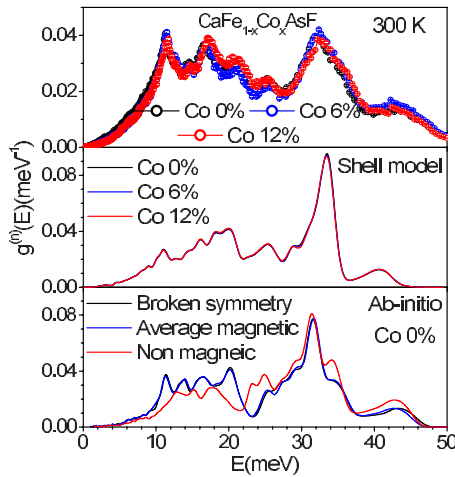


FIG. 1. (Color online) Comparison of experimental phonon spectra for $\text{CaFe}_{1-x}\text{Co}_x\text{AsF}$ ($x=0, 0.06, 0.12$). The phonon spectra are measured with incident neutron wavelength of 5.12 Å using the IN6 spectrometer at ILL. The calculated phonon spectra using the shell model and *ab initio* are also shown. The calculated spectra have been convoluted with a Gaussian of full width at half maximum (FWHM) of 5% of the energy transfer in order to describe the effect of energy resolution in the experiment.

substitution of Co at the Fe site has little effect (Figs. 1 and 3) on the phonon spectra.

Electronic-structure calculations²⁶ show that for CaFeAsF bands near the Fermi level are mainly formed by Fe 3*d* states. The substitutions of Co at the Fe site would result in an increase in electrons in the doped compound in comparison to the parent compound. Indeed there are seven electrons in the d-shell of the Co^{+2} cation, whereas the valence *d* shell of Fe^{+2} consists of six electrons. Thus the partial substitution of Co by Fe would be reflected by an increase in electronic density of states of the $\text{Fe}_{1-x}\text{Co}_x$ sublattice at the Fermi level. The changes in the electronic system upon doping may be responsible for the hardening of the low-energy modes. The

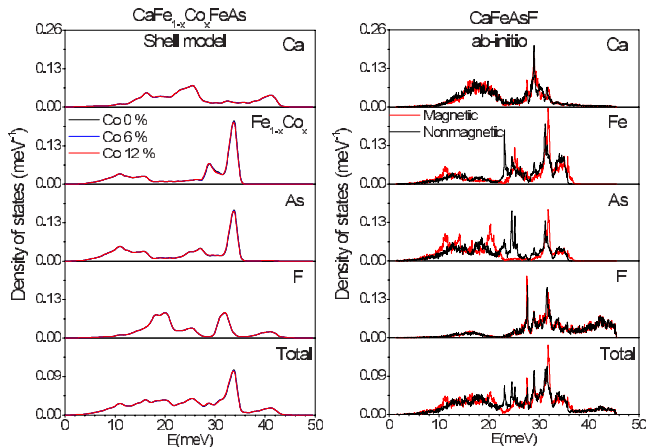


FIG. 2. (Color online) Calculated partial density of states for the various atoms in $\text{CaFe}_{1-x}\text{Co}_x\text{AsF}$ ($x=0, 0.06, 0.12$) using the shell-model and *ab initio* calculations. In the right panel, “magnetic” refers to average magnetic calculations. The spectra are normalized to unity.

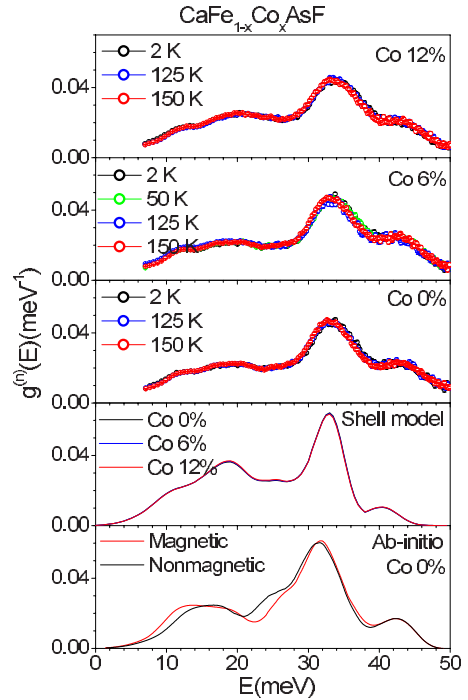


FIG. 3. (Color online) The temperature dependence of experimental phonon spectra for $\text{CaFe}_{1-x}\text{Co}_x\text{AsF}$ ($x=0, 0.06, 0.12$). The phonon spectra are measured with an incident neutron wavelength of 1.1 Å (67.6 meV) using the IN4C spectrometer at the ILL. The calculated phonon spectra using the shell model and *ab initio* are also shown. In the bottom panel, magnetic refers to average magnetic calculations. The calculated spectra have been convoluted with a Gaussian of FWHM of 4 meV in order to describe the effect of energy resolution in the experiment.

hardening can thus be taken as an indication for coupling between electrons and phonons (Fig. 1). Further increase in Co doping to 12% would further perturb the electronic density of states of $\text{Fe}_{1-x}\text{Co}_x$ at the Fermi level. The additional increase in strength of the electronic density of states may cause intermediate-energy phonons to interact with the electrons and in turn results in hardening of intermediate-energy modes (Fig. 1).

The peak in the phonon spectra resulting from the stretching vibrations of Fe-As modes remains centered at about 32 meV in all the $\text{CaFe}_{1-x}\text{Co}_x\text{AsF}$ compounds ($x=0, 0.06, 0.12$). This indicates that Fe-As bond lengths are not affected by partial substitution of Fe by Co atoms. This is what we also observe from the analysis of neutron diffraction¹⁵ on these compounds. However, the peak at about 32 meV is found to be slightly broader in Co-doped compounds in comparison with that of the parent compound. The slight distribution of Fe/Co-As bond lengths would broaden the 32 meV peak in Co-doped compounds.

When we compare these results with our previous experimental data^{22,23} of CaFe_2As_2 and $\text{Ca}_{0.6}\text{Na}_{0.4}\text{Fe}_2\text{As}_2$ compounds we find that in these compounds acoustic modes up to 12 meV do not show any change with partial doping of Na at the Ca site. The phonon modes from 12 to 40 meV in the superconducting $\text{Ca}_{0.6}\text{Na}_{0.4}\text{Fe}_2\text{As}_2$ are found to soften by about 1 to 2 meV in comparison with the parent CaFe_2As_2 .

The phonon softening in the superconducting Ca compound is attributed to the slightly longer Ca/Na-As and Fe-As bond lengths. It should be noted that in CaFe_2As_2 doping is at the Ca site, while the electronic bands near the Fermi level in CaFe_2As_2 arise mainly from the Fe and As atoms. So it is difficult to comment on the effect of change in electronic structure on the phonon modes of $\text{Ca}_{0.6}\text{Na}_{0.4}\text{Fe}_2\text{As}_2$. The situation in CaFeAsF is more favorable. We study the effect of Co doping at the Fe site on the phonon spectra. For CaFeAsF , Fe bands are mainly believed to be contributing to the superconductivity. We expect that Co doping at the Fe site would change the electronic density of states of the $\text{Fe}_{1-x}\text{Co}_x$ sublattice in the superconducting compounds in comparison with the parent CaFeAsF and this in turn could harden the acoustic and intermediate phonon spectra.

B. Temperature dependence of phonon spectra for $\text{CaFe}_{1-x}\text{Co}_x\text{AsF}$ compounds ($x=0,0.06,0.12$)

Recently we have reported neutron powder-diffraction experiments for $\text{CaFe}_{1-x}\text{Co}_x\text{AsF}$ compounds ($x=0,0.06,0.12$). Our measurements show that the parent compound CaFeAsF undergoes a tetragonal-to-orthorhombic phase transition at 134 K followed by the magnetic transition at 114(3) K while cooling the sample. The long-range antiferromagnetic order has been observed to coexist¹⁵ with superconductivity in the orthorhombic phase of the underdoped $\text{CaFe}_{0.94}\text{Co}_{0.06}\text{AsF}$ (onset $T_c=20$ K). The tetragonal-to-orthorhombic phase-transition temperature for $\text{CaFe}_{0.94}\text{Co}_{0.06}\text{AsF}$ is determined to be around 85(3) K, which is lower than that in the parent compound CaFeAsF . Magnetic order is found to be completely suppressed in optimally doped $\text{CaFe}_{0.88}\text{Co}_{0.12}\text{AsF}$ ($T_c=20$ K).

We have measured the temperature dependence of phonon spectra for the $\text{CaFe}_{1-x}\text{Co}_x\text{AsF}$ compounds ($x=0,0.06,0.12$) at 2, 125, and 150 K. For $\text{CaFe}_{0.94}\text{Co}_{0.06}\text{AsF}$ we have collected one more data set at 50 K since the tetragonal-to-orthorhombic phase transition in this compound is determined to be around 85(3) K while lowering the temperature. The temperature dependence of phonon spectra for $\text{CaFe}_{1-x}\text{Co}_x\text{AsF}$ compounds ($x=0,0.06,0.12$) is shown in Fig. 3. Phonon modes are expected to shift toward higher energies with decrease in the unit-cell volume with decreasing temperature. However our measurements show that temperature variation across the tetragonal-to-orthorhombic phase transition or magnetic-phase transition has little effect on the phonon spectra of the parent compound. It seems that the formation of Cooper pairs has no influence on the overall vibrational spectrum of $\text{CaFe}_{1-x}\text{Co}_x\text{AsF}$ compounds ($x=0.06,0.12$) across the superconducting transition temperature ($T_c=20$ K). This observation is quite similar to our earlier studies on parent and superconducting $M\text{Fe}_2\text{As}_2$ ($M=\text{Ba,Ca,Sr}$) compounds. The renormalization of specific phonons, if it exists, may however be difficult to detect in a powder sample.

The Bose-factor-corrected $S(Q,E)$ plots for $\text{CaFe}_{1-x}\text{Co}_x\text{AsF}$ compounds ($x=0,0.06,0.12$) at various temperatures measured using the IN4C spectrometer are shown in Fig. 4. Our measurements do not show any clear signa-

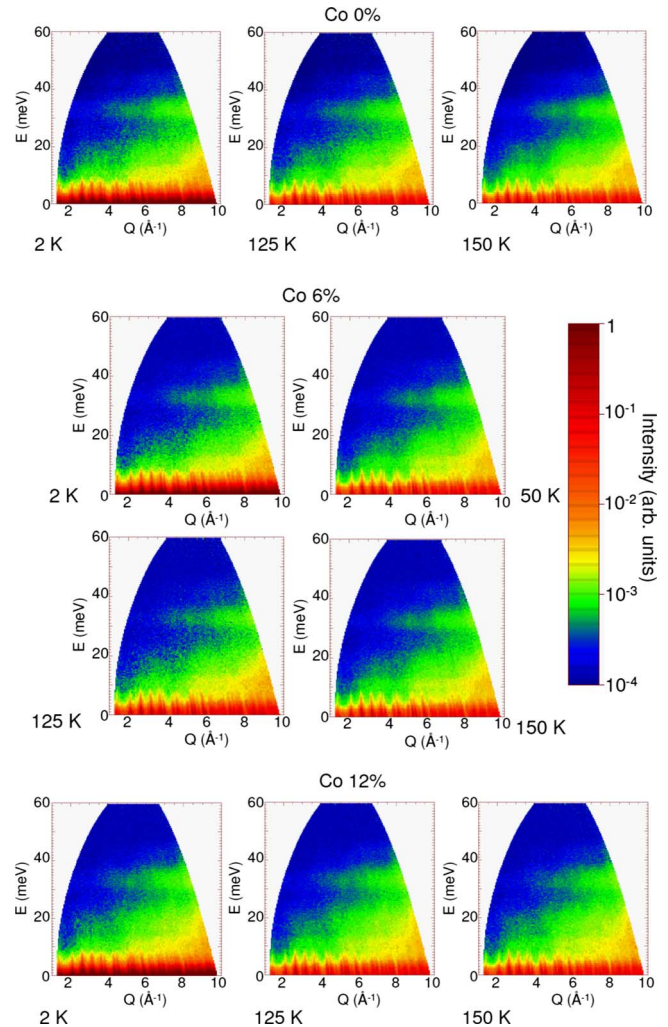


FIG. 4. (Color online) The experimental Bose factor corrected $S(Q,E)$ plots for $\text{CaFe}_{1-x}\text{Co}_x\text{AsF}$ ($x=0,0.06,0.12$) measured using the IN4C spectrometer at the ILL with an incident neutron wavelength of 1.1 Å. The values of $S(Q,E)$ are normalized to the mass of sample in the beam. For clarity, a logarithmic representation is used for the intensities.

tures of spin or resonant-spin excitations in parent and superconducting compounds, respectively, in the attainable (Q,E) range of IN4C. Recent inelastic measurements show evidence of spin¹⁶ and resonant-spin¹⁶ excitations in the antiferromagnet and superconducting state of BaFe_2As_2 and $\text{Ba}_{0.6}\text{K}_{0.4}\text{Fe}_2\text{As}$, respectively. These measurements were carried out using the MERLIN spectrometer at ISIS. The (Q,E) range attainable at IN4C is different from that of MERLIN at low Q values. Further investigations might be necessary before drawing any final conclusions concerning $\text{CaFe}_{1-x}\text{Co}_x\text{AsF}$ compounds ($x=0,0.06,0.12$).

C. Phonon calculations in $\text{CaFe}_{1-x}\text{Co}_x\text{AsF}$ compounds ($x=0,0.06,0.12$)

The experimental phonon spectra collected for $\text{CaFe}_{1-x}\text{Co}_x\text{AsF}$ compounds ($x=0,0.06,0.12$) as a function of temperature are shown in Fig. 3. The phonon spectra have

been calculated using both the shell-model and first-principles DFT-based methods. To simulate the nonstoichiometry arising from the doping the shell-model calculations are carried out for a $2 \times 2 \times 2$ supercell, where 6% and 12% of the Fe atoms are randomly replaced by Co atoms. The calculated phonon spectra (Figs. 1 and 3) for parent, 6% and 12% Co-doped compounds show little difference as discussed in detail in Sec. IV A. However experimental data for 6% and 12% Co-doped compounds show hardening of acoustic- and intermediate-energy modes in comparison with the parent compound.

In order to understand the contribution of various atomic motions to the phonon spectra we have calculated the partial densities of states (Fig. 2). The shell-model calculations show that the Fe and As atoms mainly contribute in the 0–35 meV range, while the vibrations due to Ca and F atoms contribute in the entire 0–45 meV range, respectively. The Fe-As stretching modes are above 30 meV. The estimated range of vibrational frequencies for different atoms from *ab initio* calculations is comparable with shell-model calculations except for the Ca vibrations. DFT-based calculations show vibrations in the frequency range extending up to 35 meV for Ca atoms comparable to the vibrational frequencies of Fe and As, whereas in the shell-model calculation these vibrations extend up to 45 meV.

The *ab initio* calculations (Fig. 3) are in excellent agreement with the inelastic neutron-scattering data and empirical shell-model calculations when viewed with the resolution on IN4. It is worth noting that the differences between the magnetic and nonmagnetic *ab initio* calculations appear to be small with the magnetic calculation offering slightly better agreement with the experimental data. In order to understand these differences we have calculated partial densities of states for both cases. We find that vibrations frequencies of Ca and F atoms match very well in both the magnetic and nonmagnetic calculations (Fig. 2). However, there are slight differences in the vibrations of Fe and As in both cases. The inclusion of magnetic interactions results in a shift of the peak at 12 meV to lower energies in the Fe partial density of states. However, Fe modes above 23 meV are found to harden by 1–2 meV in comparison with that of the nonmagnetic calculations. In the case of As vibrations the magnetic ordering results in softening of low-energy vibrations, as in the case of Fe atoms. This is most spectacular for modes at 25 meV which are redshifted by about 5 meV. The intermediate frequency vibrations of As atoms from 28 meV and above harden with the inclusion of magnetic ordering. The As atom vibrations are therefore a sensitive probe of the magnetic ordering in the Fe sublattice.

A more stringent check of the quality of the computed densities of states is provided by the higher resolution IN6 data in terms of spectral frequency, see Fig. 1. The relative intensities of low- and high-frequency peaks is not so well reproduced with respect to the IN6 data since the longer wavelength on this instrument tends to lead to an incomplete sampling of reciprocal space and therefore the density of states. Figure 1 shows the results of averaged magnetic interactions and precise magnetic ordering in the broken-symmetry approach. The differences between the two kinds of magnetic calculation are minor but they both offer a sig-

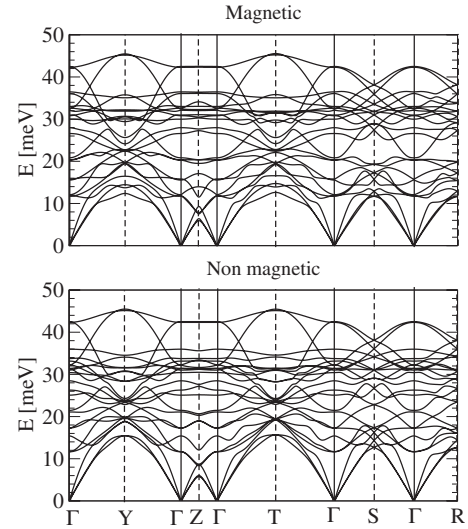


FIG. 5. Phonon dispersion relations for CaFeAsF from *ab initio* calculations. In the upper panel, magnetic refers to average magnetic calculations. The Bradley-Cracknell notation is used for the high-symmetry points along which the dispersion relations are obtained: $Y=(12,1/2,0)$, $Z=(0,0,1/2)$, $T=(1/2,1/2,1/2)$, $S=(0,1/2,0)$, and $R=(0,1/2,1/2)$.

nificant improvement over the nonmagnetic calculation, when these results are compared with the IN6 data. The similarity of the two types of magnetic calculations indicates that, although magnetic interactions have to be included in the calculation of interatomic forces, the details of magnetic ordering are less important. This is of relevance to the experimental observation (Fig. 3) that no significant changes are detected in the vibrational spectra when passing the magnetic-phase transitions in these compounds.

These differences in the partial densities of states can also be understood from the phonon-dispersion relations (Fig. 5). The comparison of the calculated dispersion relations in both the cases shows that for magnetic calculations the zone-boundary modes around 12 meV are shifted to lower energies in comparison with that of nonmagnetic calculations. Similarly, there is greater density of phonon branches in nonmagnetic calculations for energies around 23–25 meV, which results in new peak in the density of states at around 23–25 meV.

Another interesting feature to note is that the vibrational frequency range of all the atoms (Ca, Fe, As, and F) in CaFeAsF is nearly the same. This is significantly different from our previous calculations^{22,23} on CaFe₂As₂ where Ca vibrations were limited to a narrow frequency range. This shows that bonding of the Ca atom is quite different in CaFe₂As₂ and CaFeAsF compounds due to additional Ca-F interactions and consequently the interaction between the Ca and Fe-As layer is also quite different.

V. CONCLUSIONS

We have carried out systematic studies of the measurements of phonon densities of states in CaFe_{1-x}Co_xAsF compounds ($x=0,0.06,0.12$). The comparison of the phonon

spectra of superconducting and nonsuperconducting compounds shows pronounced differences. The phonon spectra of Co-doped compounds strongly react to the amount of Co substitution in the parent compound. The renormalization of phonon modes is believed to be due to electron-phonon coupling. Our results then support coupling of electrons and phonons in Co-doped CaFeAsF compounds. The calculated partial densities of states show that the range of Ca vibrations extend over the full energy range similar to Fe, As, and

F atoms. This indicates the existence of a quite different interaction between the Ca and the Fe-As layer compared to that in CaFe₂As₂. Comparison of nonmagnetic and magnetic DFT-based calculations show that magnetic interactions have to be included in the Hessian of interatomic interactions in order to reproduce the measured GDOS but that the specific details of these interactions do not have a significant impact on the GDOS, as evidenced by the similarity of the “average magnetic” and broken-symmetry models approaches.

- ¹Y. Kamihara, T. Watanabe, M. Hirano, and H. Hosono, *J. Am. Chem. Soc.* **130**, 3296 (2008).
- ²M. Rotter, M. Tegel, and D. Johrendt, *Phys. Rev. Lett.* **101**, 107006 (2008).
- ³R. Pöttgen and D. Johrendt, *Z. Naturforsch.* **63b**, 1135 (2008).
- ⁴X. C. Wang, Q. Q. Liu, Y. X. Lv, W. B. Gao, L. X. Yang, R. C. Yu, F. Y. Li, and C. Q. Jin, arXiv:0806.4688 (unpublished).
- ⁵C. Wang, L. Li, S. Chi, Z. Zhu, Z. Ren, Y. Li, Y. Wang, X. Lin, Y. Luo, S. Jiang, X. Xu, G. Cao, and Z. Xu, *EPL* **83**, 67006 (2008).
- ⁶A. J. Drew, Ch. Niedermayer, P. J. Baker, F. L. Pratt, S. J. Blundell, T. Lancaster, R. H. Liu, G. Wu, X. H. Chen, I. Watanabe, V. K. Malik, A. Dubroka, M. Roessle, K. W. Kim, C. Baines, and C. Bernhard, *Nature Mater.* **8**, 310 (2009).
- ⁷J. S. Kim, S. Khim, L. Yan, N. Manivannan, Y. Liu, I. Kim, G. R. Stewart, and K. H. Kim, *J. Phys.: Condens. Matter* **21**, 102203 (2009).
- ⁸S. Matsuishi, Y. Inoue, T. Nomura, H. Yanagi, M. Hirano, and H. Hosono, *J. Am. Chem. Soc.* **130**, 14428 (2008).
- ⁹S. Matsuishi, Y. Inoue, T. Nomura, M. Hirano, and H. Hosono, *J. Phys. Soc. Jpn.* **77**, 113709 (2008).
- ¹⁰X. Zhu, F. Han, P. Cheng, G. Mu, B. Shen, and H.-Hu Wen, *EPL* **85**, 17011 (2009); G. Wu, Y. L. Xie, H. Chen, M. Zhong, R. H. Liu, B. C. Shi, Q. J. Li, X. F. Wang, T. Wu, Y. J. Yan, J. J. Ying, and X. H. Chen, *J. Phys.: Condens. Matter* **21**, 142203 (2009).
- ¹¹M. Tegel, S. Johansson, V. Weiss, I. Schellenberg, W. Hermes, R. Poettgen, and D. Johrendt, *Europhys. Lett.* **84**, 67007 (2008).
- ¹²T. Nomura, Y. Inoue, S. Matsuishi, M. Hirano, J. E. Kim, K. Kato, M. Takata, and H. Hosono, *Supercond. Sci. Technol.* **22**, 055016 (2009).
- ¹³S. Matsuishi, Y. Inoue, T. Nomura, Y. Kamihara, M. Hirano, and H. Hosono, *New J. Phys.* **11**, 025012 (2009).
- ¹⁴P. Cheng, B. Shen, G. Mu, X. Zhu, F. Han, B. Zeng, and H.-Hu Wen, *EPL* **85**, 67003 (2009).
- ¹⁵Y. Xiao, Y. Su, R. Mittal, T. Chatterji, T. Hansen, C. M. N. Kumar, S. Matsuishi, H. Hosono, and Th. Brueckel, *Phys. Rev. B* **79**, 060504(R) (2009).
- ¹⁶R. A. Ewings, T. G. Perring, R. I. Bewley, T. Guidi, M. J. Pitcher, D. R. Parker, S. J. Clarke, and A. T. Boothroyd, *Phys. Rev. B* **78**, 220501(R) (2008); A. D. Christianson, E. A. Goremychkin, R. Osborn, S. Rosenkranz, M. D. Lumsden, C. D. Malliakas, L. S. Todorov, H. Claus, D. Y. Chung, M. G. Kanatzidis, R. I. Bewley, and T. Guidi, *Nature (London)* **456**, 930 (2008).
- ¹⁷D. J. Singh, *Phys. Rev. B* **78**, 094511 (2008); L. Boeri, O. V. Dolgov, and A. A. Golubov, *Phys. Rev. Lett.* **101**, 026403 (2008).
- ¹⁸A. P. Litvinchuk, V. G. Hadjiev, M. N. Iliev, B. Lv, A. M. Guloy, and C. W. Chu, *Phys. Rev. B* **78**, 060503(R) (2008); K.-Y. Choi, D. Wulferding, P. Lemmens, N. Ni, S. L. Bud'ko, and P. C. Canfield, *ibid.* **78**, 212503 (2008).
- ¹⁹T. Fukuda, A. Q. R. Baron, S. Shamoto, M. Ishikado, H. Nakamura, M. Machida, H. Uchiyama, S. Tsutsui, A. Iyo, H. Kito, J. Mizuki, M. Arai, H. Eisaki, and H. Hosono, *J. Phys. Soc. Jpn.* **77**, 103715 (2008); M. Le Tacon, M. Krisch, A. Bosak, J.-W. G. Bos, and S. Margadonna, *Phys. Rev. B* **78**, 140505(R) (2008).
- ²⁰D. Reznik, K. Lokshin, D. C. Mitchell, D. Parshall, W. Dmowski, D. Lamago, R. Heid, K.-P. Bohnen, A. S. Sefat, M. A. McGuire, B. C. Sales, D. G. Mandrus, A. Asubedi, D. J. Singh, A. Alatas, M. H. Upton, A. H. Said, Yu. Shvyd'ko, and T. Egami, arXiv:0810.4941 (unpublished).
- ²¹R. Mittal, Y. Su, S. Rols, T. Chatterji, S. L. Chaplot, H. Schober, M. Rotter, D. Johrendt, and Th. Brueckel, *Phys. Rev. B* **78**, 104514 (2008).
- ²²R. Mittal, Y. Su, S. Rols, M. Tegel, S. L. Chaplot, H. Schober, T. Chatterji, D. Johrendt, and Th. Brueckel, *Phys. Rev. B* **78**, 224518 (2008).
- ²³R. Mittal, S. Rols, M. Zbiri, Y. Su, H. Schober, S. L. Chaplot, M. Johnson, M. Tegel, T. Chatterji, S. Matsuishi, H. Hosono, D. Johrendt, and Th. Brueckel, *Phys. Rev. B* **79**, 144516 (2009).
- ²⁴M. Zbiri, H. Schober, M. R. Johnson, S. Rols, R. Mittal, Y. Su, M. Rotter, and D. Johrendt, *Phys. Rev. B* **79**, 064511 (2009).
- ²⁵R. Mittal, L. Pintschovius, D. Lamago, R. Heid, K.-P. Bohnen, D. Reznik, S. L. Chaplot, Y. Su, N. Kumar, S. K. Dhar, A. Thamizhavel, and Th. Brueckel, *Phys. Rev. Lett.* **102**, 217001 (2009).
- ²⁶I. R. Shein and A. L. Ivanovskii, arXiv:0810.3498 (unpublished).
- ²⁷Y. Su, P. Link, A. Schneidewind, Th. Wolf, P. Adelman, Y. Xiao, M. Meven, R. Mittal, M. Rotter, D. Johrendt, Th. Brueckel, and M. Loewenhaupt, *Phys. Rev. B* **79**, 064504 (2009).
- ²⁸T. Yildirim, *Phys. Rev. Lett.* **102**, 037003 (2009).
- ²⁹D. L. Price and K. Skold, in *Neutron Scattering*, edited by K. Skold and D. L. Price (Academic, Orlando, 1986), Vol. A; J. M. Carpenter and D. L. Price, *Phys. Rev. Lett.* **54**, 441 (1985); S. Rols, H. Jobic, and H. Schober, *C. R. Phys.* **8**, 777 (2007).
- ³⁰V. F. Sears, *Neutron News* **3**, 26 (1992); *Neutron Data Booklet*, edited by A.-J. Dianoux and G. Lander (Institut Laue-Langevin, Grenoble, France, 2002).
- ³¹A. Sjolander, *Ark. Fys.* **14**, 315 (1958).
- ³²S. L. Chaplot, N. Choudhury, S. Ghose, M. N. Rao, R. Mittal, and K. N. Prabhathasree, *Eur. J. Mineral.* **14**, 291 (2002).

- ³³R. Mittal, S. L. Chaplot, and N. Choudhury, *Prog. Mater. Sci.* **51**, 211 (2006).
- ³⁴G. Venkataraman, L. Feldkamp, and V. C. Sahni, *Dynamics of Perfect Crystals* (MIT Press, Cambridge, 1975).
- ³⁵S. L. Chaplot (unpublished).
- ³⁶P. E. Blöchl, *Phys. Rev. B* **50**, 17953 (1994).
- ³⁷P. Hohenberg and W. Kohn, *Phys. Rev.* **136**, B864 (1964).
- ³⁸W. Kohn and L. J. Sham, *Phys. Rev.* **140**, A1133 (1965).
- ³⁹G. Kresse and J. Furthmüller, *Comput. Mater. Sci.* **6**, 15 (1996).
- ⁴⁰G. Kresse and D. Joubert, *Phys. Rev. B* **59**, 1758 (1999).
- ⁴¹J. P. Perdew, K. Burke, and M. Ernzerhof, *Phys. Rev. Lett.* **77**, 3865 (1996).
- ⁴²J. P. Perdew, K. Burke, and M. Ernzerhof, *Phys. Rev. Lett.* **78**, 1396 (1997).
- ⁴³K. Parlinski, Z.-Q. Li, and Y. Kawazoe, *Phys. Rev. Lett.* **78**, 4063 (1997).
- ⁴⁴K. Parlinski, software PHONON (2003).